

Magnetic Tuning of the Relativistic BCS-BEC Crossover

Jin-cheng Wang,¹ Vivian de la Incera,² Efrain J. Ferrer,² and Qun Wang¹

¹*Interdisciplinary Center for Theoretical Study and Department of Modern Physics, University of Science and Technology of China, Hefei 230026, People's Republic of China*

²*Department of Physics, University of Texas at El Paso, El Paso, Texas 79968, USA*

The effect of an applied magnetic field in the crossover from Bose-Einstein condensate (BEC) to Bardeen-Cooper-Schrieffer (BCS) pairing regimes is investigated. We use a model of relativistic fermions and bosons inspired by those previously used in the context of cold fermionic atoms and in the magnetic-color-flavor-locking phase of color superconductivity. It turns out that as with cold atom systems, an applied magnetic field can also tune the BCS-BEC crossover in the relativistic case. We find that no matter what the initial state is at $B = 0$, for large enough magnetic fields the system always settles into a pure BCS regime. In contrast to the atomic case, the magnetic field tuning of the crossover in the relativistic system is not connected to a Feshbach resonance, but to the relative numbers of Landau levels with either BEC or BCS type of dispersion relations that are occupied at each magnetic field strength.

PACS numbers: 12.38.Mh, 03.75.Nt, 24.85.+p, 26.60.-c

I. INTRODUCTION

In recent years many experimental advances have been made in pairings of ultracold fermionic atoms, where the effective attractive interaction between the atoms can be tuned with the help of an applied magnetic field via a Feshbach resonance [1]. By tuning the fermion-fermion interaction it has been possible to experimentally realize the crossover between the weakly coupled Bardeen-Cooper-Schrieffer (BCS) superfluid regime with the formation of Cooper pairs of two fermionic atoms and the strong coupling regime where the pairs turn into difermion molecules in Bose-Einstein condensation (BEC) [2]. Even though there is no phase transition but just a crossover between these two regimes, their features are very distinct. In the BCS side the coherence length of the pairs is much larger than the mean interparticle distance and as a consequence the fermionic degrees of freedom are still manifested. However, in the BEC side, the strong interaction allows two fermions to bound into a bosonic molecule; thus no fermionic degrees of freedom remain.

The BCS-BEC crossover is not limited to cold fermionic atoms or to nonrelativistic systems. The main ingredients – a dilute gas of fermions with an attractive interaction that can favor the formation of Cooper pairs on the Fermi surface and a viable mechanism to produce the crossover – can be found in a wide range of cold and dense fermion systems. These conditions can be naturally satisfied inside the core of neutron stars, where temperatures are relatively low compared to densities which can reach values several times the normal nuclear density and hence allow deconfinement. The conditions for a BCS-BEC crossover can also be expected to be met in the planned low-energy experiments at the Relativistic Heavy Ion Collider (RHIC) and future facilities all over the world, such as the Facility for Antiproton and Ion Research (FAIR) [3], the Nuclotron-Based Ion Collider Facility (NICA), or the Japan Proton Accelerator Research

Complex (J-PARC) [4].

In recent years, interest has been spurred in investigating the realization of the BCS-BEC crossover in various QCD-inspired models [5]-[13]. A strong motivation for this activity is the need to explore the QCD-phase map at intermediate densities and low temperatures, a region of significant relevance for the physics of compact stars but inaccessible with lattice QCD due to the complex fermion determinant. The phase of QCD at asymptotically high baryonic densities is well established to be a color superconducting (CS) phase [14]. This CS phase is the result of the attractive color force in the antitriplet channel for two quarks which favors the formation of Cooper pairs on the Fermi surface. However, as the density decreases, the quark-gluon interaction becomes stronger leading to a reduction of the coherence length of the diquark pairs. What happens at this point is still a matter of debate. Some model calculations [15]-[16] suggest that the quark matter might go directly to a chirally broken hadronic phase via a strong first-order transition. Another possibility is that the diquark pairs turn first into diquark molecules, thereby undergoing a BCS-BEC crossover [11, 17]. Eventually, the diquark pair may pick up yet another quark to form a color-singlet baryon. Hence, the BCS-BEC crossover could hold the key to our understanding of the transition from CS to hadronic matter. In 1999 Schafer and Wilczek [18] conjectured that the transition from CS to hadronic matter should be actually a crossover. The quark-hadron continuity has been studied in terms of the spectral continuity of Nambu-Goldstone modes [7] and vector mesons [8]. The role of diquarks in baryon formation and dissociation in cold dense quark/nuclear matter has been recently studied in Ref. [12].

Up to now, nevertheless, one ingredient has been left out in all the investigations of the CS-hadronic matter transition via a BCS-BEC crossover: an external magnetic field. However, magnetic fields are endemic in neutron stars. Pulsars' magnetic fields range between

10^{12} and 10^{13} G [19], and for magnetars they can be as large as $10^{14} - 10^{16}$ G [20] on the surface and presumably much larger in the core. Upper limit estimates for neutron star magnetic fields indicate that their magnitude can reach $\sim 10^{18} - 10^{20}$ G [21]-[22]. Very strong magnetic fields, $\sim 10^{18}$ G/ 10^{19} G, are also generated in heavy-ion collisions at RHIC and LHC [23]. Nonetheless, these experiments produce a hot and low-density matter that is far from the QCD-phase region where the BCS-BEC crossover is expected to occur. On the other hand, as already mentioned, the future low-energy experiments at RHIC, NICA and FAIR [3]-[4] have been designed to probe the phase diagram of nuclear matter at intermediate-to-large baryon density and low temperature. These experiments are expected to produce also very strong magnetic fields [24], hence they will be relevant for understanding the field's influence on the CS-hadronic transition.

Because of the astrophysical relevance, and also in preparation for those future experiments, it is important to have a good theoretical understanding of the magnetic field effects on the CS-hadronic matter crossover. The present paper is a first attempt in this direction. It is remarkable that the identification between the low-energy theories of the hadronic matter and the color-flavor-locking (CFL) phase [18], which served as the base for the quark-hadronic matter continuity conjecture, was later found to exist too in an external magnetic field [25]. In this case the identification was between the low-energy modes of the magnetic CFL (MCFL) phase [25] and those of the hadronic matter in a magnetic field [26]. We hope that the results of the present paper will shed some light on the quark-hadronic matter crossover in the presence of a magnetic field.

The most important outcome of this work is the discovery of a new mechanism by which a magnetic field can tune the BCS-BEC crossover. The mechanism is related to the filling (emptying) of new Landau levels (LLs) when the field is varied and to the relative numbers of occupied LLs with either BEC or BCS type of dispersion relations at a given magnetic field value. The filling (emptying) of new LLs with varying field is also responsible for the de Haas-van Alphen oscillations of the gap [27]-[29] and number densities. No matter what the initial state of the system is at $B = 0$, for large enough magnetic fields the system will always reach a pure BCS regime.

Even though our calculation is based on a simple model, it encompasses the properties of spin-zero CS that are essential for the new tuning mechanism to work, mainly that the pairing fermions carry opposite charges (equivalent to the rotated charge in CFL and 2SC) to ensure the coupling of these fermions with the external field, and the lack of a Meissner effect. Moreover, the field-induced tuning mechanism is model-independent. The crossover to the BCS regime at strong field strengths occurs because at those fields most of the fermions will lie in their lowest Landau level (LLL) and the dispersion relation of the LLL quasiparticles in the paired system

is always of BCS type. Notice that this mechanism is different from the Feshbach resonance that produces the crossover in cold atom systems [30] by tuning the effective interaction between the fermions.

The plan of the paper is the following. In Sec. II we introduce the model and derive the gap and chemical equilibrium equations. In Sec. III we present our numerical results and discuss their meaning, as well as the physical origin of the crossover at large magnetic fields. The concluding remarks are given in Sec. IV.

II. RELATIVISTIC FERMION-BOSON MODEL IN A MAGNETIC FIELD

To explore the effects of the magnetic field on the BCS-BEC crossover, we will extend the model of fermions and scalar bosons interacting via a Yukawa term considered in [10], to allow for two oppositely charged fermions $\Psi^T = (\psi_1, \psi_2)$ that couple to an external, uniform and constant magnetic field B . The symmetry group of the model is $U(1)_B \otimes U(1)_{em}$, with subscripts "B" and "em" labeling the groups of baryonic and electromagnetic transformations respectively. The charged fermions in our model mimic the rotated charged quarks that pair to form neutral Cooper pairs in the CFL and 2SC phases. The theory is described by the Lagrangian density

$$\mathcal{L} = \mathcal{L}_f + \mathcal{L}_b + \mathcal{L}_I, \quad (1)$$

with

$$\mathcal{L}_f = \bar{\Psi}(i\gamma^\mu \partial_\mu + \mu\gamma^0 - \hat{Q}\gamma^\mu A_\mu - m)\Psi, \quad (2a)$$

$$\mathcal{L}_b = (\partial_\mu + 2i\mu\delta_{\mu 0})\varphi^*(\partial^\mu - 2i\mu\delta^{\mu 0})\varphi - m_b^2\varphi\varphi^*, \quad (2b)$$

$$\mathcal{L}_I = \varphi\bar{\Psi}_C(i\gamma_5\hat{G})\Psi + \varphi^*\bar{\Psi}(i\gamma_5\hat{G})\Psi_C. \quad (2c)$$

Here m and m_b denote the fermion and boson masses respectively. The charge-conjugate fermions are described by $\Psi_C = C\bar{\Psi}^T$ with $C = i\gamma^2\gamma^0$, and the electric charge $\hat{Q} = q\sigma_3$ and Yukawa coupling $\hat{G} = g\sigma_2$ operators are given in terms of the Pauli matrices σ_i . A_μ is the vector potential associated with the external magnetic field B , which, without loss of generality, can be chosen along the x_3 axis.

The Lagrangian (1) is invariant under the $U(1)_B$ transformation $\Psi \rightarrow \Psi' = e^{-i\alpha}\Psi$, $\varphi \rightarrow \varphi' = e^{i2\alpha}\varphi$. Hence the bosons carry twice the baryon number of the fermions. As in Ref. [10], chemical equilibrium with respect to the conversion of two fermions into one boson and vice versa is ensured by introducing fermion chemical potentials μ for fermions and 2μ for bosons. The transition can then be described from a weakly coupled and neutral Cooper pair of two fermions with opposite electric charges into a molecular difermionic bound state, with an electrically neutral, strongly coupled, bosonlike behavior. In order

to describe the BEC of these molecules, we have to separate the zero mode of the boson field φ and replace it by its expectation value $\phi \equiv \langle \varphi \rangle$, which represents the electrically neutral difermion condensate. The mean-field effective action is then

$$I^B(\bar{\psi}, \psi) = \frac{1}{2} \int d^4x d^4y \bar{\Psi}_{\pm}(x) \mathcal{S}_{(\pm)}^{-1}(x, y) \Psi_{\pm}(y) + (4\mu^2 - m_b^2) |\phi|^2 + |(\partial_t - 2i\mu)\varphi|^2 - |\nabla\varphi|^2 - m_b^2 |\varphi|^2, \quad (3)$$

where the fermion inverse propagators of the Nambu-Gorkov positive and negative charged fields $\Psi_+ = (\psi_2, \psi_{1C})^T$ and $\Psi_- = (\psi_1, \psi_{2C})^T$ are given by

$$\mathcal{S}_{(\pm)}^{-1} = \begin{pmatrix} [G_{(\pm)0}^+]^{-1} & i\gamma^5 \Delta^* \\ i\gamma^5 \Delta & [G_{(\pm)0}^-]^{-1} \end{pmatrix}, \quad (4)$$

with

$$[G_{(\pm)0}^{\pm}]^{-1}(x, y) = [i\gamma^\mu \Pi_\mu^{(\pm)} - m \pm \mu\gamma^0] \delta^4(x - y), \quad (5)$$

and $\Pi_\mu^{(\pm)} = i\partial_\mu \pm qA_\mu$. We take the external vector potential in the Landau gauge $A_2 = Bx_1$, $A_0 = A_1 = A_3 = 0$. The Bose condensate ϕ is related to the difermion condensate through $\Delta = 2g\phi$.

The zero temperature effective potential obtained from (3) becomes, after using Ritus's transformation to momentum space [31],

$$\Omega = -\frac{qB}{2\pi^2} \sum_{e=\pm 1} \sum_{k=0}^{\infty} d(k) \int_0^{\infty} dp_3 \epsilon_e + \frac{(m_b^2 - 4\mu^2)\Delta^2}{4g^2} + \frac{1}{4\pi^2} \sum_{e=\pm 1} \int_0^{\infty} \omega_e p^2 dp, \quad (6)$$

where $d(k) = (1 - \frac{\delta_{k0}}{2})$ denotes the spin degeneracy of the Landau levels. The energy dispersions for fermions and bosons are

$$\epsilon_e(k) = \sqrt{(\epsilon_k - e\mu)^2 + \Delta^2}, \quad e = \pm 1 \quad (7a)$$

and

$$\omega_e = \sqrt{p^2 + m_b^2} - 2e\mu, \quad e = \pm 1 \quad (7b)$$

respectively. Index k denotes the Landau level, e labels quasiparticle/antiquasiparticle contributions, and

$$\epsilon_k = \sqrt{p_3^2 + 2|qB|k + m^2}, \quad k = 0, 1, 2, \dots \quad (7c)$$

is the energy of a free fermion in a magnetic field. As always occurs with charged fermions in a magnetic field, the transverse component of the momentum is quantized (Landau levels), so the 4-momentum of the fermion in the chosen gauge is given by $\bar{p} \equiv (p_0, 0, -sgn(qB)\sqrt{|2qB|k}, p_3)$ and the energy depends

only on the longitudinal component p_3 (for a field parallel to x_3) and the Landau level k .

To investigate the crossover we first need to find the gap and chemical potential that simultaneously solve the gap equation and the condition of chemical equilibrium at fixed parameters, and then use them to obtain the density fractions of fermions and bosons as functions of the field.

Chemical equilibrium requires

$$n = n_F + n_0 \quad (8)$$

where n plays the role of a fixed total baryon number density, $n = -\partial\Omega/\partial\mu$, and the fermion number density n_F and condensate density n_0 , are respectively given by

$$n_F = -\frac{qB}{4\pi^2} \sum_{e=\pm 1} \sum_{k=0}^{\infty} ed(k) \int_0^{\infty} dp_3 \frac{\epsilon_k - e\mu}{\epsilon_e}, \quad (9)$$

$$n_0 = \frac{2\mu\Delta^2}{g^2}. \quad (10)$$

The gap equation is given by $\partial\Omega/\partial\Delta = 0$, which can be obtained from (6) as

$$\frac{\tilde{m}_b^2 - 4\mu^2}{2g^2} = \frac{qB}{2\pi^2} \sum_{e=\pm 1} \sum_{k=0}^{\infty} d(k) \int_0^{\infty} dp_3 \frac{1}{\epsilon_e(k)} - 2 \int \frac{d^3p}{(2\pi)^3} \frac{1}{\sqrt{p^2 + m^2}}. \quad (11)$$

As discussed in [10], the crossover parameter in the present case can be defined by $x \equiv -\frac{\tilde{m}_b^2 - 4\mu^2}{2g^2}$, which is linked to the renormalized boson mass \tilde{m}_b in vacuum

$$\tilde{m}_b^2 = m_b^2 - 4g^2 \int \frac{d^3p}{(2\pi)^3} \frac{1}{\sqrt{p^2 + m^2}}. \quad (12)$$

The parameter x can then be changed by hand to mimic the effect of a change in the coupling.

Since the momentum integral and the summation over fermion Landau levels are divergent, we introduce a Gaussian regulator $\exp[-(p_3^2 + 2|qB|k)/\Lambda^2]$ with momentum cutoff $\Lambda = 1$ GeV. Following the derivations of [10], one can see that at zero magnetic field the parameters of the theory g , n , m , and \tilde{m}_b can be always chosen to have $x = 0$ coinciding with the situation where the density fractions of fermions $\rho_F = n_F/n$, and bosons $\rho_{b0} = n_0/n$ are all equal to 1/2. With such a choice, and according to the criterion used in [10], negative values of x with large moduli describe a pure BCS state, large positive values of x describe a pure BEC phase, and $1/x$ plays the role of the scattering length. The selection of the model parameters can be done at any given magnetic field value, to have $x = 0$ corresponding to the unitarity limit, at which the scattering length becomes infinite. In this work, however, we are more interested in exploring the situation where we keep fixed values of the parameters, and instead change the strength of the magnetic field to

see if it can have any effect in the BCS-BEC crossover. Henceforth we will use $m = 0.2$ GeV and $g = 1$ in all the calculations¹.

III. RESULTS AND DISCUSSION

Let us discuss now the numerical solutions of Eqs. (8) and (11), along with the field dependence of the physical quantities of the problem. In Fig. 1, we set the magnetic field to three values $B = 0, 10^{19}, 2 \times 10^{19}$ G and study the influence of the field on various quantities by tuning the renormalized boson mass \tilde{m}_b . Notice that for a fixed cutoff Λ , changing the renormalized boson mass, is equivalent to changing the bare boson mass m_b .

The upper panel in Fig.1 shows the variations of the chemical potential and gap solutions with the boson mass at different field values. Even though at zero and nonzero magnetic fields the chemical potential increases and the gap decreases with m_b , a large magnetic field yields slightly smaller gap values for the same m_b in the large m_b region. For the three field strengths, the system is in a BEC state at $m_b \simeq 0.35$ GeV in the left end region of the middle panel graph, where the BEC-like pairing dominates over the BCS-like one, as reflected in the density fractions, large ρ_{b0} and small ρ_f . When m_b increases, the fermion number fraction becomes larger and finally dominates at the right end indicating a BCS regime. The system then undergoes a crossover from BEC to BCS with increasing m_b . Notice that the BCS-BEC crossover is realized in a similar way at zero and nonzero magnetic fields. However, the external magnetic field tends to favor BCS over BEC. When B is large enough ($\gtrsim 10^{19}$ G), the crossover point shifts to a lower m_b and the system is in the BCS side for a much larger set of m_b values. This strong magnetic field effect will become even more apparent in the plots of Figs. 2 and 3. The lowest panel in Fig. 1 shows the variation of the parameter x with m_b at the three field values.

Figures 2 and 3 present the behavior of different parameters as functions of the magnetic field when the system starts at zero field either in a BEC regime (Fig. 2) or in a BCS one (Fig. 3). The gap and the chemical potential solved from the gap and density equations at zero magnetic field are $\Delta_0 = 0.073$ GeV and $\mu_0 = 0.357$ GeV for $m_b = 0.8$ GeV ($\tilde{m}_b = 0.692$ GeV), and $\Delta_0 = 0.029$ GeV and $\mu_0 = 0.555$ GeV for $m_b = 1.2$ GeV ($\tilde{m}_b = 1.131$ GeV). In both cases the system ends up in the BCS regime at strong fields. As shown in Fig. 2, the influence of the magnetic field on the crossover is more

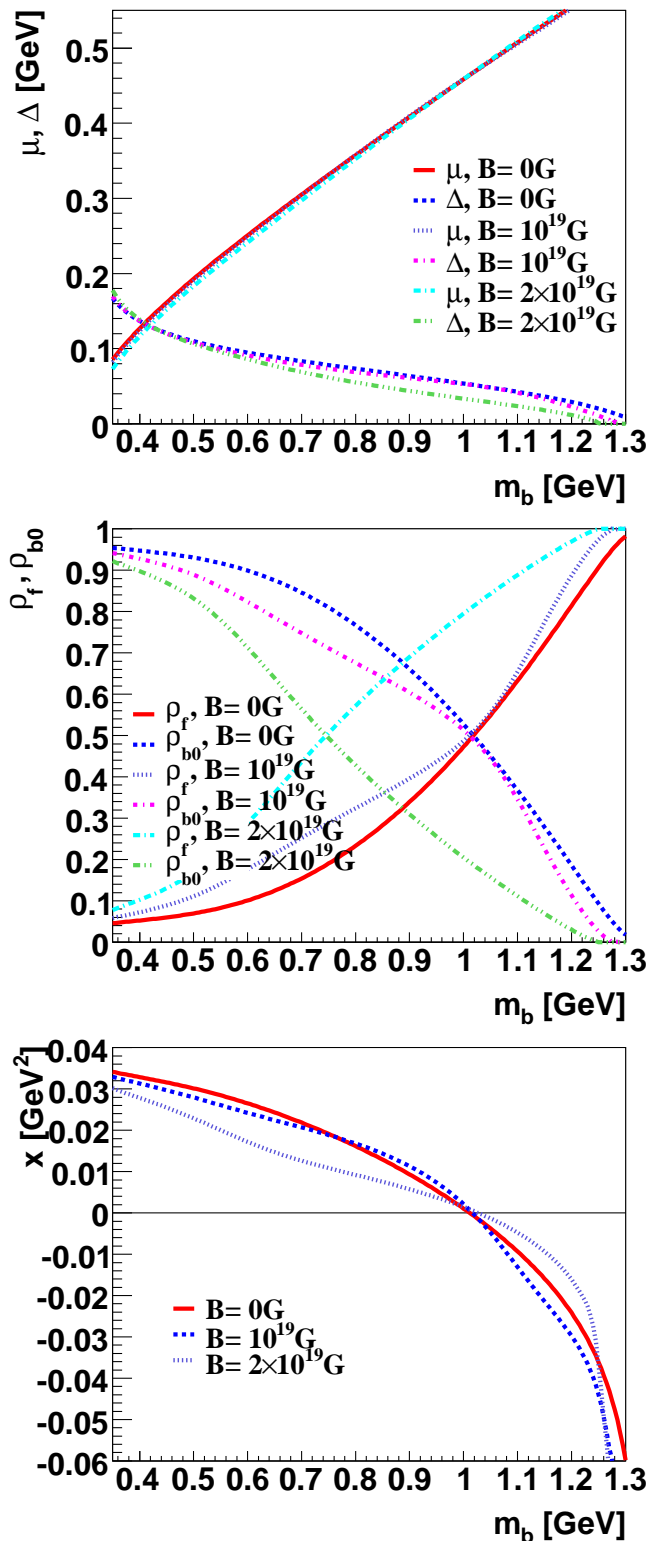


FIG. 1: Various quantities as functions of m_b at three values of the magnetic field, $B = 0, 10^{19}, 2 \times 10^{19}$ G: gap and fermionic chemical potential (upper panel), fermion and boson number fractions (middle panel), the parameter x (lower panel). The cross point is shifted by the magnetic field, as shown in the middle panel. The system starts on the BEC side and crosses over to the BCS side when m_b increases.

¹ Although we are using a toy model as a first attempt to study the field effects on the crossover, the parameters of our model are consistent with the region of low temperatures and intermediate densities, where the coupling is expected to be relatively strong and chiral symmetry breaking can in principle coexist with color superconductivity [32].

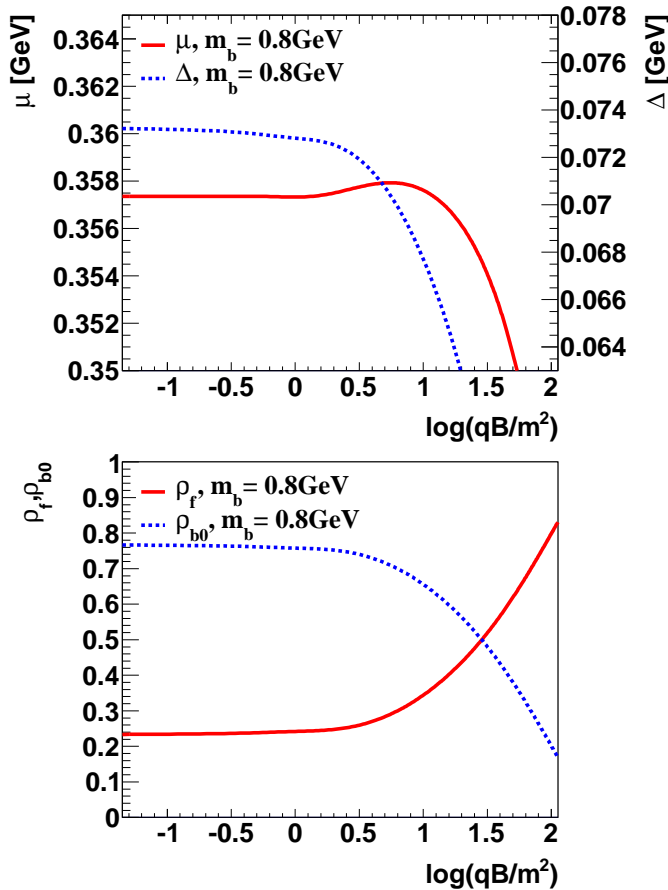


FIG. 2: Various quantities as functions of $\ln(|qB|/m^2)$: gap and fermion chemical potential (upper panel), fermion and boson number fractions (lower panel). Starting from a BEC regime, on which the BEC component is much larger than the BCS one at small fields on the left, the system crosses over to a pure BCS state at large magnetic fields on the right. The scale of the field-induced oscillations is too small to be visible in the plot.

dramatic when the system starts in the BEC side, as reflected in the behavior of the number fractions shown in the lower panel of that figure. On the other hand, when the system is in the BCS regime at $B = 0$ (Fig. 3) the applied magnetic field simply strengthens the nature of that regime. The de Haas-van Alphen oscillations displayed by the physical parameters in the two panels of Fig. 3 have been also obtained in other models of color superconductivity in a magnetic field [29]. The oscillations also exist in Fig. 2, but their scale is smaller and hence are not visible in the plots. The scale of the oscillations is connected to the magnitude of the gap. The larger the m_b , the smaller the gap magnitude and hence, the larger the amplitude of the field-induced oscillations.

The origin of the crossover to a pure BCS state at large fields can be understood in terms of the behavior of the fermion quasiparticle dispersion relations (7). To see this, let us introduce the LL-dependent mass square $M_k^2 \equiv 2|qB|k + m^2$ in terms of which the quasiparticle

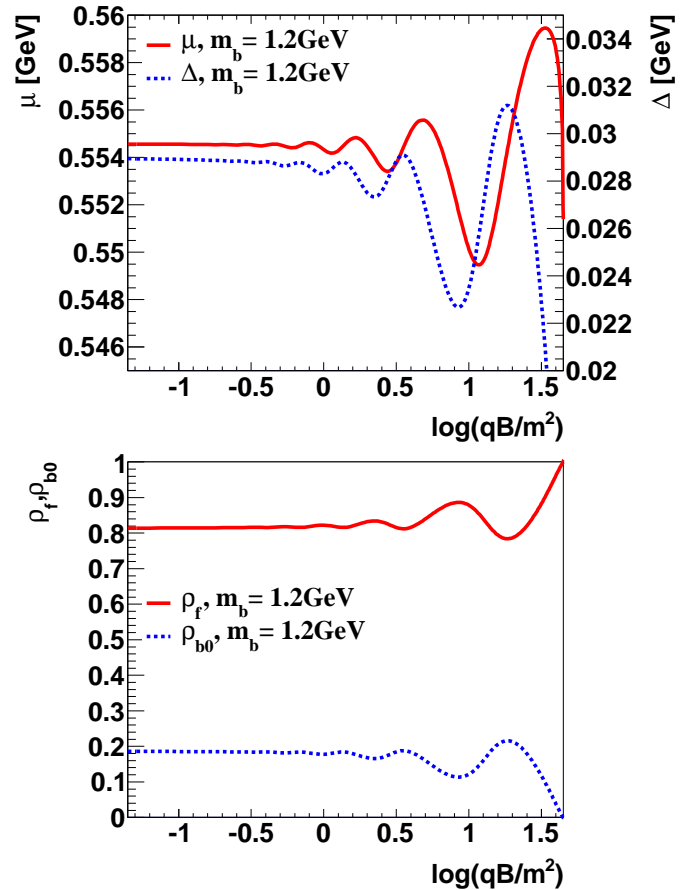


FIG. 3: Same as Fig. 2 except that the starting state has an excess of BCS pairing over BEC pairing at small magnetic field. The magnetic field induces the de Haas-van Alphen oscillations in all the physical quantities with larger amplitudes than in Fig. 2 because the gap is smaller in this case. The oscillations stop when the field is large enough to put all the fermions in the LLL ensuring a pure BCS state.

dispersion becomes

$$\epsilon_+(k) = \sqrt{(\sqrt{p_3^2 + M_k^2} - \mu)^2 + \Delta^2}. \quad (13)$$

Notice that for all the LLs satisfying the condition $\mu > M_k$, the minimum of the dispersion $\epsilon_+(k)$ occurs at $p_3 = \sqrt{\mu^2 - M_k^2}$, with excitation energy given by the gap Δ , a behavior characteristic of the BCS regime. On the other hand, for LLs with $\mu < M_k$, the minimum of $\epsilon_e(k)$ occurs at $p_3 = 0$, with excitation energy $\sqrt{(\mu - M_k)^2 + \Delta^2}$, typical of the BEC regime. Therefore, the BCS-BEC crossover in the presence of the magnetic field is controlled by the relative numbers of LLs for which the sign of the effective chemical potential $\mu_k = \mu - M_k$ is either positive (BCS type) or negative (BEC type). In other words, all the LLs up to certain $k_{BCS} = N$, such that $M_N < \mu < M_{N+1}$, produce fermionlike modes and thus contribute to the BCS component, while all the LLs with $k > k_{BCS}$ produce bosonlike modes, hence contributing

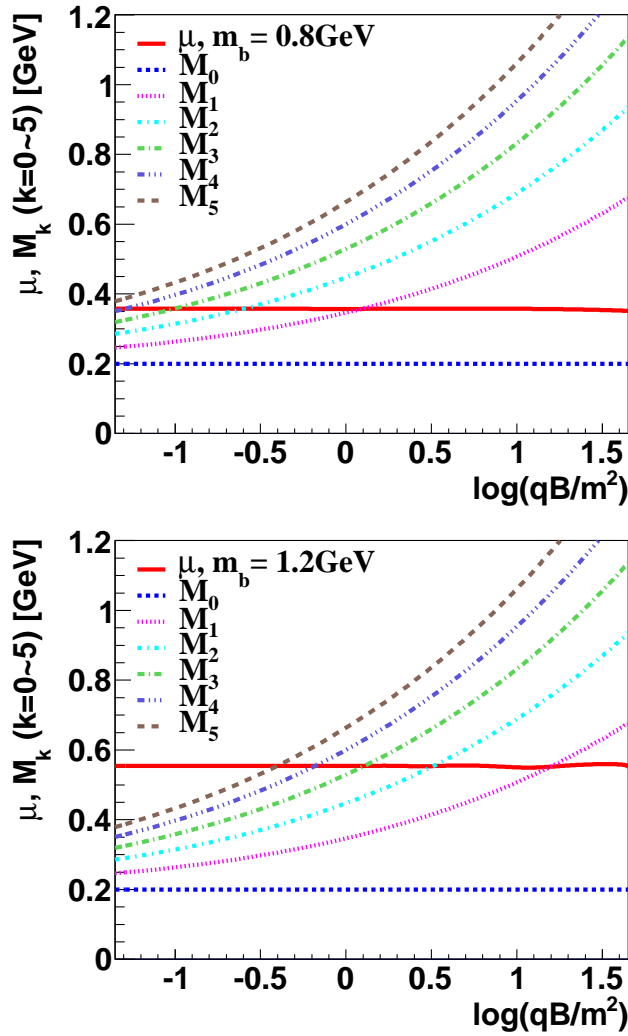


FIG. 4: Variation of the quasiparticles' effective masses of the first few Landau levels with the magnetic field. The solid (red) line represents the chemical potential. Masses over this line give rise to a bosonlike dispersion, those below the line to a fermionlike one. The upper (lower) panel corresponds to the case where the system starts in the BEC (BCS) regime at zero field.

to the BEC one. When the field changes, the effective mass M_k changes, as does the total number of LLs contributing to Eqs. (8) and (11) and the density of states of each LL. This leads to oscillations in the chemical potential μ that in turn are reflected in the number of LLs contributing to each regime. At fields large enough to put all the fermions in the LLL, one has $M_k = m$ and the dispersion reduces to

$$\epsilon_+(0) = \sqrt{(\sqrt{p_3^2 + m^2} - \mu)^2 + \Delta^2}, \quad (14)$$

thus the system is in the BCS regime, as long as $\mu > m$. Therefore, a strong enough magnetic field will ultimately favor the crossover to a BCS regime.

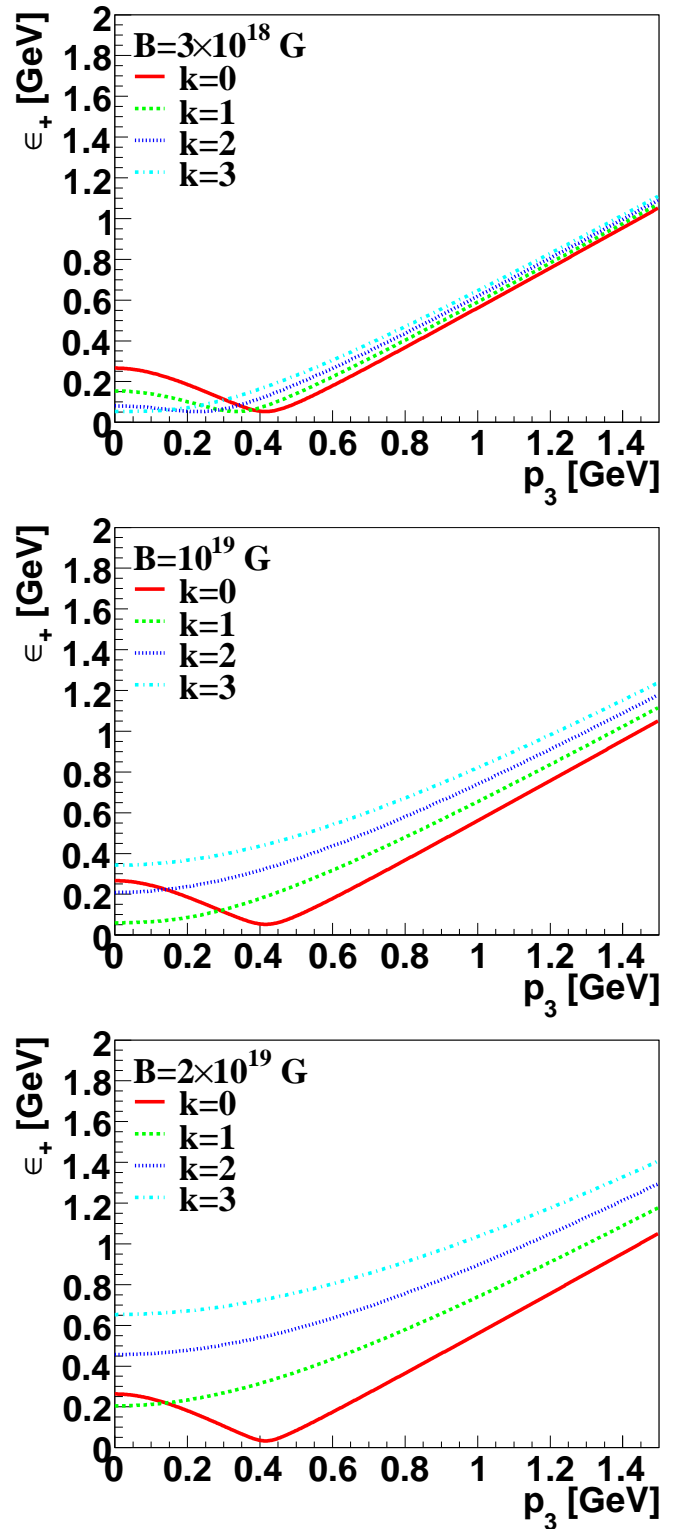


FIG. 5: Fermion dispersion relations at three fixed values of magnetic field, $3 \times 10^{18} \text{G}$, 10^{19}G and $2 \times 10^{19} \text{G}$. $k = 0, 1, 2, 3$ denote the Landau levels. The boson mass m_b is set to 1 GeV.

Figure 4 shows the consistency of the above interpretation. In this figure we plotted the chemical potential μ and the effective mass M_k of a few LLs as functions of the magnetic field when the system starts at zero field in the BEC regime (upper panel), or in the BCS one (lower panel). At low fields, the effective masses of all the LLs in the lower panel lie below μ , indicating the predominance of the BCS-type modes (positive μ_k), in agreement with the low-field behavior depicted in Fig. 3 for the same value of m_b . In contrast, the effective masses of most of the LLs in the upper panel either lie over μ at low fields or cross the μ line at much smaller field values than in the lower panel case, because the system is throughout this entire small-field range in the BEC side, in agreement with the behavior shown in Fig. 2. When the field increases the levels start to cross the μ line, but at the same time the higher LLs start to empty because the density of states of each level increases with the field and hence the lower levels can accommodate more and more fermions. Finally, when the magnetic and the Fermi energies become comparable, $|qB| \geq \mu^2$, all the fermions lie in the LLL with a BCS-like dispersion because $M_0 < \mu$. Therefore, in the strong field region, all the modes are LLL modes and the two systems lie deep in the BCS regime. This is the basis of the field-induced crossover mechanism.

We call to the reader's attention that, on a closer look, the essence of the above description of a field-induced relativistic BCS-BEC crossover is not too different from the essence of the crossover at zero field previously studied in other systems, relativistic [33] and nonrelativistic [34]. In the nonrelativistic case [34], the crossover can be induced by the change in the sign of the chemical potential with increasing coupling that leads to a change in the character of the system from fermionic ($\mu > 0$) to bosonic ($\mu < 0$). In a similar fashion, the crossover in the relativistic system considered in [33] is driven by the charge density change and controlled by the sign of the parameter $\mu - m$ rather than μ itself [33]. Notice that what the magnetic field does in the relativistic case studied in the present paper is to introduce a new energy scale in the system, $\sqrt{|qB|}$, which enters in the effective chemical potential μ_k . Then the sign of μ_k and the number of LLs with each sign serve to control the crossover. The system will be in: a) a BCS state if the majority of occupied LLs have $\mu_k > 0$, b) a BEC state if the majority of LL have $\mu_k < 0$, or c) in the crossover region if the numbers of LLs with positive and negative μ_k are comparable.

In Fig. 5 we show the dispersion relations for quasi-particles ϵ_+ for different LLs at three magnetic fields' values. In the upper panel of Fig. 5, the LLs with $k < 3$ contribute to the BCS component, while the one with $k = 3$ contributes to the BEC one. Since the fermion energy splitting between different LLs and the density of states of each LL are each proportional to \sqrt{eB} , when the field increases not only do the levels become more separated in energy, as seen from the figure, but also they can accommodate a larger number of particles. As a conse-

quence, when the field increases, the number of occupied LLs reduces. This means that the higher levels shown in the middle and lower panels of Fig. 5 are likely not contributing already at those strong fields.

IV. CONCLUDING REMARKS

In this paper we investigated the effect of a magnetic field in the relativistic BCS-BEC crossover in the context of a model with neutral bosons and charged fermions minimally coupled to a magnetic field. The simple model used in our calculations resembles some basic properties of spin-zero color superconducting phases in a magnetic field like for instance the MCFL phase [25].

Our results demonstrate that a magnetic field can tune the BCS-BEC crossover via a novel mechanism according to which the state of the system at each field is determined by the number of occupied LLs with either positive or negative effective chemical potential $\mu_k = \mu - M_k$. If the majority of the LLs have $\mu_k < 0$, the system is in a BEC state, because a majority of BEC-type modes prevails. On the contrary, if the majority of the LLs have $\mu_k > 0$, it is in the BCS regime. At strong enough fields, the system goes to the BCS regime, because in this case only the LLL, whose dispersion is always of BCS type, is occupied.

The BCS-BEC crossover has been studied in the literature using two types of models: single-channel models and two-channel models. In two-channel models, like the one used in this paper, fermion and boson degrees of freedom are introduced from the beginning in the Lagrangian. In single-channel models one starts with a Lagrangian that only has fermionic degrees of freedom, like in a Nambu-Jona-Lasinio (NJL) model. Then, the bosonic degrees of freedom are introduced with the help of a bosonization procedure as the Hubbard-Stratonovich transformation. A natural continuation of the present work will be to investigate the magnetic field effect on the crossover in the context of a single-channel theory. Given that the dispersions of the charged fermions in the presence of a magnetic field will be of the same form in a purely fermionic theory in the presence of a magnetic field, one can still use the sign of the effective chemical potential μ_k and the relative numbers of LLs with each sign as valid criteria to control the crossover.

There are different NJL theories that could be used as single-channel models. One interesting possibility would be to consider the field effects in a NJL model with both diquark and chiral condensates that can interact via the axial anomaly, such as the one considered in [13]. We could then explore how the field-induced crossover mechanism found in our two-channel model turns out to be in this case, where the mass of the charged fermions is not necessarily constant, but can itself be affected by the field in any region where the diquark and chiral condensates coexist.

Apart from the obvious fundamental motivation of un-

derstanding the effects of a magnetic field in the BCS-BEC crossover within a more realistic model, if the relativistic BCS-BEC theories discussed in the literature have any relevance for the physics of neutron stars and the future low-energy, heavy-ion collision experiments, it makes sense to consider them with a magnetic field, as extremely strong magnetic fields are expected to be present in these two settings. Therefore, an imperative next step will be to consider more realistic models of color super-

conducting quark matter to explore all the implications of a magnetic field in the BCS-BEC crossover.

Acknowledgments: The work of VI and EJJ has been supported in part by DOE Nuclear Theory Grant No. de-sc0002179. QW is supported in part by the "100 talents" project of the Chinese Academy of Sciences (CAS) and by the National Natural Science Foundation of China (NSFC) under Grant No. 10735040.

-
- [1] K. M. O'Hara *et al.*, *Science* **298**, 2179 (2002); A. Simoni *et al.*, *Phys. Rev. Lett.* **90**, 163202 (2003); S. Gupta *et al.*, *Science* **300**, 1723 (2003); C. A. Regal *et al.*, *Nature (London)* **424**, 47 (2003); J. Cubizolles *et al.*, *Phys. Rev. Lett.* **91**, 240401 (2003); K. E. Strecker *et al.*, *Phys. Rev. Lett.* **91**, 080406 (2003); S. Jochim *et al.*, *Phys. Rev. Lett.* **91**, 240402 (2003).
- [2] S. Jochim *et al.*, *Science* **302**, 2101 (2003); M. Greiner *et al.*, *Nature (London)* **426**, 537 (2003); M. Zwierlein *et al.*, *Phys. Rev. Lett.* **91**, 250401 (2003).
- [3] P. Senger, T. Galatyuk, A. Kiseleva, D. Kresan, A. Lebedev, S. Lebedev and A. Lymanets, *J. Phys. G* **36**, 064037 (2009).
- [4] K. Fukushima and T. Hatsuda, arXiv:1005.4814[hep-ph], 2010.
- [5] Y. Nishida and H. Abuki, *Phys. Rev. D* **72**, 096004 (2005); A. H. Rezaeian, H. J. Pirner, *Nucl. Phys. A* **779**, 197 (2006); L. He and P. Zhuang, *Phys. Rev. D* **76**, 056003 (2007); G.-F. Sun, L. He, and P. Zhuang, *Phys. Rev. D* **75**, 096004 (2007); H. Abuki, *Nucl. Phys. A* **791**, 117 (2007); M. Kitazawa, D. H. Rischke and I. A. Shovkovy, *Phys. Lett. B* **663**, 228 (2008); H. Abuki and T. Brauner, *Phys. Rev. D* **78**, 125010 (2008); J. Deng, J.-C. Wang and Q. Wang, *Phys. Rev. D* **78**, 034014 (2008); D. Blaschke, and D. Zablocki, *Phys. Part. Nucl.* **39**, 1016 (2008); T. Brauner, *Phys. Rev. D* **77**, 096006 (2008); J. O. Andersen, *Nucl. Phys. A* **820**, 171C (2009); H. Guo, C.-C. Chien, and Y. He, *Nucl. Phys. A* **823**, 83 (2009); B. Chatterjee, H. Mishra, and A. Mishra, *Phys. Rev. D* **79**, 014003 (2009).
- [6] T. Hatsuda *et al.*, *Phys. Rev. Lett.* **97**, 122001 (2006).
- [7] N. Yamamoto *et al.*, *Phys. Rev. D* **76**, 074001 (2007).
- [8] T. Hatsuda, M. Tachibana, and N. Yamamoto, *Phys. Rev. D* **78**, 011501 (2008).
- [9] N. Yamamoto and T. Kanazawa, *Phys. Rev. Lett.* **103**, 032001 (2009).
- [10] J. Deng, A. Schmitt and Q. Wang, *Phys. Rev. D* **76**, 034013 (2007).
- [11] H. Abuki, G. Baym, T. Hatsuda and N. Yamamoto, *Phys. Rev. D* **81**, 125010 (2010).
- [12] J.-C. Wang, Q. Wang, and D. H. Rischke, arXiv:1008.4029 [nucl-th].
- [13] H. Basler and M. Buballa, *Phys. Rev. D* **82**, 094004 (2010).
- [14] M. Alford, K. Rajagopal and F. Wilczek, *Phys. Lett. B* **422**, 247 (1998); *Nucl. Phys. B* **537**, 443 (1999); R. Rapp, T. Schafer, E. V. Shuryak, and M. Velkovsky, *Phys. Rev. Lett.* **81**, 53 (1998); D. T. Son, *Phys. Rev. D* **59**, 094019 (1999); R. D. Pisarski and D. H. Rischke, *Phys. Rev. D* **61**, 074017 (2000); W. E. Brown, J. T. Liu and H. C. Ren, *Phys. Rev. D* **61**, 114012 (2000).
- [15] M. Asakawa and K. Yazaki, *Nucl. Phys. A* **504**, 668 (1989).
- [16] J. Berges and K. Rajagopal, *Nucl. Phys. B* **538**, 215 (1999).
- [17] M. Matsuzaki, *Phys. Rev. D* **62**, 017501 (2000); H. Abuki, T. Hatsuda, and K. Itakura, *Phys. Rev. D* **65**, 074014 (2002); K. Itakura, *Nucl. Phys. A* **715**, 859 (2003).
- [18] T. Schafer and F. Wilczek, *Phys. Rev. Lett.* **82**, 3956 (1999).
- [19] J. H. Taylor *et al.*, *Astrophys. J. S* **88**, 529 (1993); A. G. Lyne, F. Graham-Smith, *Pulsar Astronomy* (Cambridge Univ. Press., Cambridge, 2005).
- [20] B. Paczynski, *Acta Astron.* **42**, 145 (1992); C. Thompson and R. C. Duncan, *ApJ* **392**, L9 (1992); **473**, 322 (1996); A. Melatos, *Astrophys. J. Lett.* **519**, L77 (1999).
- [21] L. Dong and S. L. Shapiro *ApJ* **383**, 745 (1991).
- [22] E. J. Ferrer *et al.*, *Phys. Rev. C* **82**, 065802 (2010); L. Paulucci *et al.*, *Phys. Rev. D* **83**, 043009 (2011).
- [23] V. V. Skokov, A. Yu. Illarionov and V. D. Toneev, *Int. J. Mod. Phys. A* **24**, 5925 (2009).
- [24] V. D. Toneev and V. Voronyuk, arXiv:1011.5589v1 [nucl-th] 2010.
- [25] E. J. Ferrer, V. de la Incera and C. Manuel, *Phys. Rev. Lett.* **95**, 152002 (2005); *Nucl. Phys. B* **747**, 88 (2006); E. J. Ferrer and V. de la Incera, *Phys. Rev. D* **76**, 045011 (2007).
- [26] V. A. Miransky, I. A. Shovkovy, *Phys. Rev. D* **66**, 045006 (2002).
- [27] W. J. de Haas and P. M. van Alphen, *Leiden Commun. A* **212**, 215 (1930); *Proc. R. Acad. Sci. Amsterdam*, **33**, 1106 (1930);
- [28] D. Ebert *et al.*, *Phys. Rev. D* **61**, 025005 (1999).
- [29] J. L. Noronha and I. A. Shovkovy, *Phys. Rev. D* **76**, 105030 (2007); K. Fukushima and H. J. Warringa, *Phys. Rev. Lett.* **100**, 032007 (2008); B. Feng, E. J. Ferrer and V. de la Incera, "Cooper Pair's Magnetic Moment in MCFL Color Superconductivity" arXiv:1012.3204 [nucl-th], *Nucl. Phys. B* (in press) doi:10.1016/j.nuclphysb.2011.07.016
- [30] W. C. Stwalley, *Phys. Rev. Lett.* **37**, 1628 (1976); E. Tiesinga, B. J. Verhaar, and H. T. C. Stoof, *Phys. Rev. A* **47**, 4114 (1993).
- [31] V. I. Ritus, *Ann. Phys.* **69**, 555 (1972); *Sov. Phys. JETP* **48**, 788 (1978) [*Zh. Eksp. Teor. Fiz.* **75**, 1560 (1978)]; E. Elizalde, E. J. Ferrer, and V. de la Incera, *Ann. of Phys.* **295**, 33 (2002); E. Elizalde, E. J. Ferrer, and V. de la Incera, *Phys. Rev. D* **70**, 043012 (2004). C. N. Leung and S.-Y. Wang *Nucl. Phys. B* **747**, 266 (2006).

- [32] S.B. Ruester *et al.*, Phys. Rev. D **72**, 034004 (2005);
H. Abuki and T. Kunihiro, Nucl. Phys. A **768**, 118
(2006).
- [33] G. Sun, L. He and P. Zhuang, Phys.Rev.D **75**, 096004
(2007).
- [34] Q. Chen, J. Stajic, S. Tan and K. Levin, Phys Rept. **412**,
1 (2005).